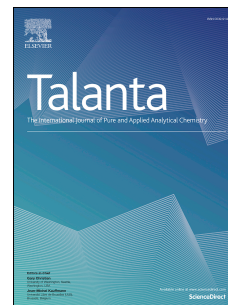


Journal Pre-proof

Microwave-sustained inductively coupled atmospheric-pressure plasma (MICAP) for the elemental analysis of complex matrix samples

Raquel Serrano, Guillermo Grindlay, Luis Gras, Juan Mora



PII: S0039-9140(24)00045-6

DOI: <https://doi.org/10.1016/j.talanta.2024.125666>

Reference: TAL 125666

To appear in: *Talanta*

Received Date: 15 October 2023

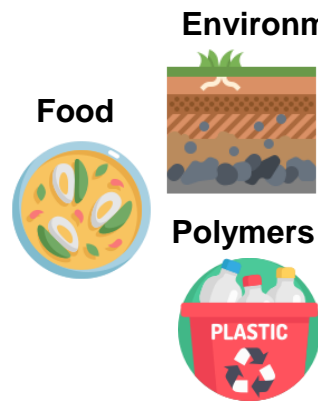
Revised Date: 23 December 2023

Accepted Date: 12 January 2024

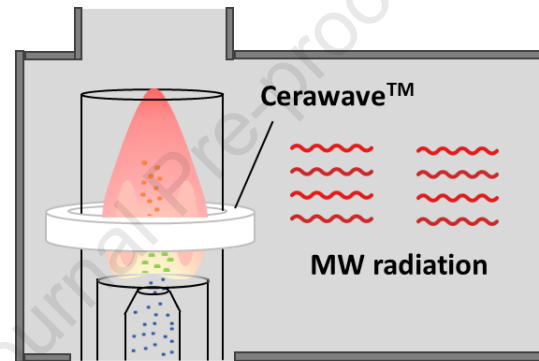
Please cite this article as: R. Serrano, G. Grindlay, L. Gras, J. Mora, Microwave-sustained inductively coupled atmospheric-pressure plasma (MICAP) for the elemental analysis of complex matrix samples, *Talanta* (2024), doi: <https://doi.org/10.1016/j.talanta.2024.125666>.

This is a PDF file of an article that has undergone enhancements after acceptance, such as the addition of a cover page and metadata, and formatting for readability, but it is not yet the definitive version of record. This version will undergo additional copyediting, typesetting and review before it is published in its final form, but we are providing this version to give early visibility of the article. Please note that, during the production process, errors may be discovered which could affect the content, and all legal disclaimers that apply to the journal pertain.

© 2024 Published by Elsevier B.V.

COMPLEX MATRIX SAMPLES

Digestion/
Extraction

**MICAP-OES**

- ✓ Accuracy and precision
- ✓ Real-time IS correction
- ✓ Inorganic acid and organic solutions do not cause significant matrix effects
- ✓ Straightforward optimization to mitigate EIEs matrix effects

Microwave-sustained inductively coupled atmospheric-pressure plasma (MICAP) for the elemental analysis of complex matrix samples.

Raquel Serrano, Guillermo Grindlay, Luis Gras, Juan Mora

Department of Analytical Chemistry, Nutrition and Food Sciences, University of Alicante, PO Box 99, 03080 Alicante, Spain.

E-mail: Raquel.serrano@ua.es

Abstract

Microwave induced plasma optical emission spectrometry (MIP-OES) has gained widespread attention in the last few years for trace elemental analysis. Among the new generation of MIPs it is worth to mention the microwave-sustained inductively coupled atmospheric-pressure plasma (MICAP) for which previous works have shown similar detection capabilities to those afforded by ICP-OES. Nevertheless, this instrument has not been applied yet to complex matrix sample analysis. Therefore, the goal of this work is to evaluate MICAP-OES performance (e.g., analytical figures of merit, matrix effects, etc.) for elemental analysis of samples of different nature (e.g., environmental, food and polymers). To this end, both spectral and non-spectral interferences were investigated for 19 elements (Ag, Al, As, B, Ca, Cd, Co, Cr, Cu, Fe, Ga, In, Mg, Mn, Ni, Pb, Sr, Tl, Zn) in the presence of inorganic acid, organic and saline solutions and compared to a 5% w w⁻¹ HNO₃ solution. Unlike previous MIPs, experimental data showed that the

optimum nebulizer gas flow rate for a given emission wavelength was mostly independent of matrix characteristics. Regarding matrix effects, this device was highly robust operating both inorganic acid and organic matrices. Interestingly, when operating saline matrices, changes on emission signal by easily ionizable elements were less significant than those early reported by alternative MIP cavities. Moreover, due to MICAP spectrometer design employed allows real-time simultaneous analysis, Rh, Pd, Sc and Y were suitable internal standards to minimize non-spectral interferences. Finally, MICAP-OES can be successfully applied to the elemental analysis of different complex matrix samples (i.e., CRM-DW1 Drinking water; BCR-146 Sewage sludge industrial; BCR-185 Bovine liver; BCR-278R Mussel tissue; NIST-1549 Non-fat milk powder; ERM-EC681k Polyethylene (high level) and BCR-483 Sewage sludge amended soil).

Keywords: microwave plasma, optical emission spectrometry, metals, environmental, food, polymers

1 1. Introduction

2 Inductively coupled plasma optical emission spectrometry (ICP-OES) is the
3 workhorse technique for trace elemental analysis in many areas due to its
4 outstanding multi-elemental detection capabilities and limits of detection (LoD) at
5 $\mu\text{g L}^{-1}$ levels. Nonetheless, microwave induced plasma optical emission
6 spectrometry (MIP-OES) has been gaining popularity as an alternative technique
7 to ICP-OES for trace element analysis. New instrumental developments (i.e.,
8 cavity designs, high-powered magnetrons, etc.) has dramatically improved
9 technique analytical figures of merit, being limits of detection for most metals on
10 a par with those afforded by ICP-OES.[1,2] In addition, one of the most attractive
11 features of current MIP-OES instrumentation is the use of either nitrogen or air
12 for plasma generation, thus reducing significantly operating costs with regard
13 ICP-OES which requires argon instead. Therefore, MIP-OES instruments have
14 been successfully applied for the analysis of samples of very different
15 composition (environmental,[3,4] clinical,[5] food,[6,7] beverages,[8]
16 petrochemical,[9,10] and ethanol-containing samples,[11] among others). For a
17 detailed description of the state-of-the-art readers are referred to the reviews by
18 Muller et al. [1] and Fontoura et al. [2]

19 Though recent technical advances of MIP-OES, the development of
20 analytical procedures with this technique is still complex since: (i) the nebulizer
21 gas flow (Q_g) affects differently atomic and ionic emission lines which complicates
22 the optimization of the experimental conditions;[12,13] (ii) matrix effects are still
23 significant for samples containing easily ionizable elements (i.e., Na, Ca, Mg,
24 etc.);[14,15,16]. For instance, signal changes up to 5 and 7-fold have been

25 reported when operating 0.25 mol L⁻¹ NaNO₃ and 0.25 mol L⁻¹ CaCl₂ solutions
26 [13] and; (iii) sample throughput is significantly reduced because most
27 instruments make use of sequential spectrometers. Recently, a new MIP cavity
28 design has been developed by Jevtic et al. [17,18,19,20] termed microwave-
29 sustained inductively coupled atmospheric-pressure plasma (MICAP). This new
30 cavity uses a ceramic dielectric resonator ring (Cerawave™) that plays the same
31 role as the traditional ICP load coil. When this device is subjected to a microwave
32 field (2.45 GHz) a magnetic field is generated capable of supporting an annular
33 nitrogen plasma as that obtained with ICPs. Analytical capabilities of this new
34 atomization source have been evaluated for both optical emission (OES)
35 [21,22,23] and mass spectrometry (MS) [24] providing equivalent analytical
36 figures of merit to those afforded by alternative high-power (N₂)-MIP cavities and
37 argon ICP.[22] Recently, it has been demonstrated that soils [25] and steel [26]
38 samples can be satisfactorily analysed by means of MICAP-MS avoiding the
39 typical Ar-based polyatomic interferences that affect some isotopes (e.g., As, Ca,
40 Cr, Mn, Fe) in ICP-MS. Nevertheless, the feasibility of using MICAP-OES for the
41 analysis of samples with complex matrices have not been reported yet. The lack
42 of technical applications may be attributable to the fact that MICAP has been
43 recently developed and therefore deep-knowledge of matrix effects with this
44 system as well as the appropriate calibration strategies (internal standardization,
45 matrix-matching, standard addition, etc.) to overcome them are limited. It must
46 be considered that even though previous fundamental studies about matrix
47 effects by saline matrices in MICAP-OES have demonstrated a clear advance in
48 the knowledge of the behaviour of this cavity [21,27] they cannot be directly

49 extrapolated to routine applications because the concentrations tested are not
50 comparable to those usually employed for real sample preparation.[4,13]
51 Consequently further studies on this regard are required if the MICAP is going to
52 be applied for the analysis of real samples showing complex matrices.[13,16]

53 Thus, the aim of the present study is to evaluate the analytical capabilities of
54 MICAP-OES for trace elemental determination in real sample analysis. To this
55 end, both spectral and non-spectral interferences were systematically
56 investigated for 19 elements (Ag, Al, As, B, Ca, Cd, Co, Cr, Cu, Fe, Ga, In, Mg,
57 Mn, Ni, Pb, Sr, Tl, Zn) in the presence of acid, organic and saline solutions since
58 they are usually employed in sample preparation (digestion and extraction) or
59 even they are naturally present in real samples. Next, the selection of plasma
60 experimental conditions and calibration strategies were examined. Finally, the
61 developed procedure was validated by analysing seven certified reference
62 materials (i.e., environmental, food, and polymers).

63

64 **2. Experimental**

65 **2.1 Reagents**

66 Deionised water produced in a Millipore (Paris, France) Milli-Q device was
67 used to prepare the solutions employed throughout this work. Suprapure nitric
68 acid 69% w w⁻¹, sulfuric acid 98% w w⁻¹, hydrochloric acid 37% w w⁻¹, acetic acid
69 glacial 99.7% w w⁻¹, calcium chloride 6-hydrate 98% w w⁻¹, and sodium nitrate
70 99% w w⁻¹ were purchased from Panreac (Barcelona, Spain).
71 Ethylenediaminetetraacetic acid (EDTA) 98.5% w w⁻¹, glycerol 86-88% w w⁻¹,
72 1000 mg L⁻¹ mono-elemental solutions (As, Au, P, Pd, Rh, Sb, Sc, Sn, Ti, V and

73 Y) and 1000 mg L⁻¹ multi-elemental ICP-IV solution (Ag, Al, B, Ba, Bi, Ca, Cd, Co,
74 Cr, Cu, Fe, Ga, In, K, Li, Mg, Mn, Na, Ni, Pb, Sr, Tl, and Zn) were obtained from
75 Sigma-Aldrich (Steinheim, Germany).

76

77 **2.2 Matrix and analyte solutions**

78 Multielemental solutions containing 50 mg kg⁻¹ of each analyte (Ag, Al, As, B,
79 Ca, Cd, Co, Cr, Cu, Fe, Ga, In, Mg, Mn, Ni, Pb, Sr, Tl, and Zn) were prepared in
80 six different matrix solutions: (i) 20 g L⁻¹ S (prepared from sulfuric acid); (ii) 20 g
81 L⁻¹ Cl (prepared from hydrochloric acid); (iii) 20 g L⁻¹ C (prepared from glycerol);
82 (iv) 10 g L⁻¹ C (equivalent to a 0.43 mol L⁻¹ HOAc prepared from acetic acid
83 glacial); (v) 0.10 mol L⁻¹ Na (prepared from NaNO₃); and (vi) 0.25 mol L⁻¹ Ca
84 (prepared from calcium chloride 6-hydrate). For the sake of comparison, a 5% w
85 w⁻¹ nitric acid multielemental solution has been employed as a reference. The
86 concentrations of the solutions were expressed in mol L⁻¹ or g L⁻¹ unit to facilitate
87 the comparison of the data obtained in the present work with those data
88 previously reported in the literature. Inorganic acids such as sulfuric acid [28] and
89 hydrochloric acid were selected since they are usually employed in sample
90 preparation (e.g., sample storage and acid digestion treatments) [29,30] whereas
91 the use of acetic acid, EDTA and saline matrices in the indicated concentrations
92 were commonly used in different elemental bioavailability extraction methods
93 (e.g., BCR sequential extraction methodology, single-step extraction) [31,32] for
94 the analysis of trace elements in soils and sediments.

95

96 **2.3 MICAP instrumentation**

97 MICAP-OES measurements were performed using a MICAP-OES 1000
98 device designed by Radom corporation (Pewaukee, USA), which comprises
99 independent plasma and spectrometer units coupled with a fiber optic
100 connection. The former device consists of an aluminium waveguide that contains
101 a 1.0 kW magnetron to generate the microwave field, an inductive iris to provide
102 impedance matching, the dielectric resonator ring (Cerawave™) and the torch
103 assembly. For all the experiments, a Fassel type quartz torch (20 mm) with a 1.5
104 mm diameter injector installed vertically (axial view) was used. The sample
105 introduction system employed consisted of a OneNeb® concentric pneumatic
106 nebulizer (Ingeniatrics, Sevilla, Spain) coupled to a cyclonic spray chamber. On
107 the other hand, the spectrometer contains an echelle grating (slit width 30 μm)
108 which allows to simultaneously measure of the entire wavelength range (194-625
109 nm), and a Peltier-cooled charge-coupled device (sCCD) detector (resolution
110 2048-2048; pixel size: 11 μm x 11 μm). Instrument operating conditions and
111 emission wavelengths monitored through this work are, respectively, gathered in
112 Table 1 and Table S1 (Supplementary material). The later includes spectroscopic
113 information about analyte atomic and ionic emission lines (i.e. upper electronic
114 level involved in each electron transition, $E_{\text{upper level}}$) molecular emission bands to
115 assess plasma status (N_2^+ 391.439 nm) and internal standards (Au, Pd, Rh, Sc
116 and Y) used to mitigate potential matrix effects by sample concomitants.

117

118 **2.4 Samples**

119 To evaluate the strengths and weakness of MICAP-OES for real sample
120 analysis, seven certified reference materials (CRM) were analysed to cover

121 **Table 1.** MICAP-OES operating conditions.

MICAP-OES	
Plasma forward power (W)	1000
Plasma gas (L min ⁻¹)	14
Auxiliary gas (L min ⁻¹)	0.4
Nebulizer gas (Q _g) (L min ⁻¹)	0.3-0.9
Sample uptake rate (Q _i) (mL min ⁻¹)	0.3
Sample introduction system:	
Nebulizer	OneNeb [®]
Spray chamber	Cyclonic (inner volume 42 cm ³)
View mode	Axial
Integration time (s)	1
Replicates	3

122

123 different kind of samples and matrix concomitants (e.g., environmental, food and
 124 polymer samples). The certified reference materials selected were: (i) CRM-DW1
 125 Drinking water; (ii) BCR-146 Sewage sludge industrial; (iii) BCR-185 Bovine liver;
 126 (iv) BCR-278R Mussel tissue; (v) NIST-1549 Non-fat milk powder; (vi) ERM-
 127 EC681k Polyethylene (high level); and (vii) BCR-483 Sewage sludge amended
 128 soil. All samples, except the drinking water and the polyethylene, were oven-dried
 129 at 60 °C until constant weight. After that, samples were sieved to <2.0 mm and
 130 stored in properly named polyethylene bottles until treatment.

131

132

133 *2.4.1 Sample digestion*

134 For the determination of the total elemental concentration, the drinking water
 135 sample was analysed directly, and the other certified reference materials were
 136 digested in triplicate using a Milestone S.r.l. (Soriso, Italy) Ultrawave oven at

137 conditions recommended by the manufacturer (Table S2). For BCR-146 Sewage
138 sludge industrial, BCR-185 Bovine liver, BCR-278R Mussel tissue and NIST-
139 1549 Non-fat milk powder digestions, 4 mL of HNO₃ 65% w w⁻¹ were added to
140 0.1 g of sample in Teflon vessels, whereas for ERM-EC681k Polyethylene (high
141 level), 4 mL of HNO₃ 65% w w⁻¹ and 1 mL of H₂SO₄ 98% w w⁻¹ were added to 0.1
142 g of sample. After the digestion process samples were transferred to polyethylene
143 bottles and brought to a final weight of 15 g with ultrapure water and filtered using
144 a syringe filter of 0.45 µm pore size. Finally, samples were stored at 4°C until
145 analysis by MICAP-OES.

146

147 2.4.2 Extraction procedures

148 For the elemental bioavailability extraction procedure, the BCR-483 Sewage
149 sludge amended soil was used in four different single step extractions carried out
150 as indicated in Table S3 using the extractions solutions recommended in the
151 CRM report (i.e., 0.05 mol L⁻¹ EDTA, 0.43 mol L⁻¹ HOAc, 0.01 mol L⁻¹ CaCl₂ and
152 0.1 mol L⁻¹ NaNO₃). After each single step extraction, samples were centrifuged
153 and filtered using a syringe filter of pore size 0.45 µm. Finally, solutions were
154 stored in polyethylene vials at 4°C until analysis by MICAP-OES.

155

156

157 3. Results and discussion

158 Analytical capabilities of MICAP-OES in combination with commercially
159 available spectrometers have been previously reported in the literature mainly for
160 some aqueous [23], organic [22] and saline matrices. [21,22] Nevertheless,

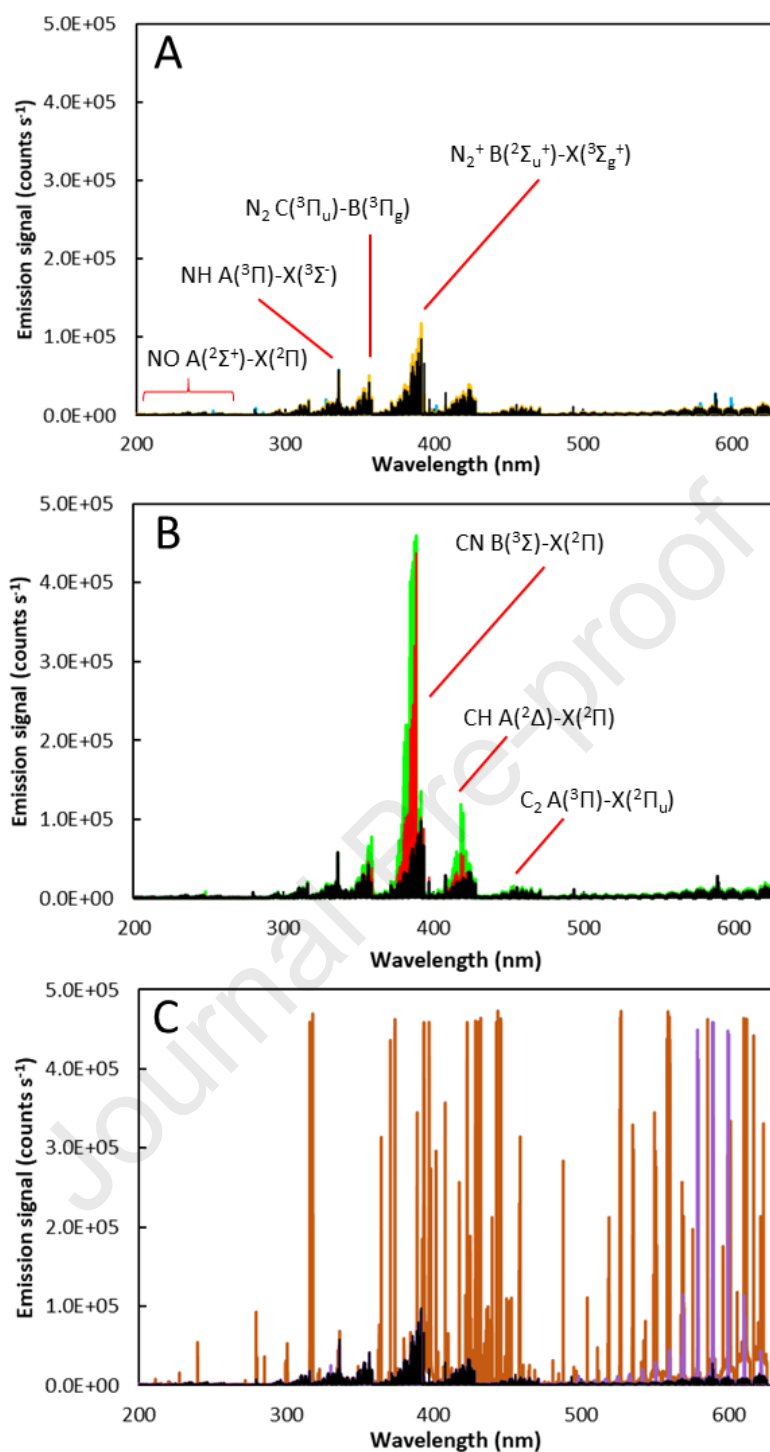
161 matrix effects caused by matrices with concentration and composition
162 comparable to those commonly found in sample analysis have not been
163 evaluated yet. Thus, in the present study, three different types of matrices: (i)
164 inorganic acids (i.e., H₂SO₄ and HCl); (ii) organic matrices (i.e., glycerol and
165 acetic acid) and; (iii) saline matrices (i.e., Na and Ca concomitants) have been
166 selected to assess spectral and non-spectral interferences. In all cases, a 5% w
167 w⁻¹ nitric acid solution was selected as a reference since it is usually used for
168 sample digestion and conservation and its physicochemical properties are similar
169 to water standards.[33] In this work, a sample introduction system composed by
170 a Oneneb[®] nebulizer and a cyclonic spray chamber was selected to minimize
171 matrix effects on aerosol generation and transport thus allowing to evaluate the
172 role of the plasma discharge on both spectral and non-spectral interferences.
173 [12,13,34]. A plasma power of 1000 W was employed through this work since the
174 MICAP does not allow to modify this parameter. On the other hand, sample
175 uptake rate was fixed at 0.3 mL min⁻¹ since there is no signal improvement using
176 higher values (Fig S1). Consequently, the influence of Q_g on both background
177 and analyte emission was specifically investigated.

178

179 **3.1 Spectral interferences**

180 The background profile and the possible occurrence of additional emission
181 lines and molecular emission bands due to the incomplete atomization of the
182 matrices selected in the plasma were evaluated. The emission spectra were
183 monitored in the 194-625 nm wavelength range. Fig. 1 shows the emission
184 spectra obtained at an intermediate Q_g (0.5 L min⁻¹) for each group of matrices

185 (i.e., (A) acid; (B) organic and; (C) saline solutions) along with that obtained for
186 the reference solution, 5% w w⁻¹ nitric acid solution (black line). As expected from
187 previous studies with the MICAP and alternative (N₂)-MIP cavities and
188 MICAP,[22,35] background spectra for the reference solution was dominated by
189 molecular bands from different nitrogen-based species (Fig. 1A), namely: (i) NO
190 (180-280 nm, B(²Π)-X(²Π)); (ii) NH (336 nm, A(²Σ⁺)-X(²Π)); and (iii) N₂⁺ (390
191 nm,(B(²Σ_u⁺)-X(³Σ_g⁺)).[36] Non-significant differences in background emission
192 spectral were found between inorganic acids (Fig. 1A) and the reference matrix.
193 Additional molecular emission bands and peaks were, however, observed for
194 organic (Fig. 1B) and saline solutions (Fig. 1C). For the former (i.e., 20 g L⁻¹ C
195 and 10 g L⁻¹ C) (Fig. 1B), it is interesting to note, that and increase in the N₂⁺ band
196 was noticed. This enhancement was not related to an improvement of N₂
197 ionization, but mainly with a spectral interference caused by CN emission band
198 at 388.340 nm (B(²Σ)-X(²Π)) which saturates the detector operating the 20 g L⁻¹
199 C solution. On this regard, additional carbon-based molecular emission bands
200 appeared at wavelength higher than 388 nm related to the carbon-based
201 molecular species CH 431.420 nm (A(²Δ)-X(²Π)) and C₂ 473.700 nm (A(³Π)-
202 X(²Π_u)). [36,37] Irrespective of the carbon source employed (i.e., glycerol or
203 acetic acid), carbon-based molecular emission band intensities followed the order
204 CN>CH>C₂.



205

206 **Fig. 1** Background emission spectra for (A) inorganic acid (i.e., 20 g L⁻¹ Cl (blue) 20 g L⁻¹ S (yellow)); (B) organic (i.e., 10 g L⁻¹ C (red) and 20 g L⁻¹ C (green)); and (C) saline matrices (i.e., 0.25 mol L⁻¹ Ca (orange) and 0.10 mol L⁻¹ Na (purple)). Background spectrum for the 5% w w⁻¹ nitric acid reference solution is shown in black. Q_g 0.5 L min⁻¹; Q_l 0.3 ml min⁻¹.

211

212 Moreover, as expected from its carbon concentration, the 20 g L⁻¹ C solution
213 afforded higher emission signal for the carbon-based molecular species than the
214 10 g L⁻¹ C one. On the other hand, in the presence of the saline matrices (Fig.
215 1C) a complex background was recorded for 0.25 mol L⁻¹ Ca matrix due to the
216 appearance of different atomic and ionic Ca emission lines [38] as well as to the
217 elemental impurities commonly present in calcium salts (i.e., Sr, Mg, etc.). Similar
218 findings were noticed for the 0.10 mol L⁻¹ Na matrix but in these case Na atomic
219 and ionic emission lines were specifically located in the 500-600 nm wavelength
220 range.

221 Because background emission is strongly correlated to solvent load and
222 plasma characteristics,[12] additional experiments were carried out using
223 alternative Q_g values (i.e., 0.3 L min⁻¹ - 0.9 L min⁻¹). The results obtained (Fig. S2)
224 shown that, in general, the background emission signal decreased with the
225 increase of Q_g for all the matrices with the exception of the 0.25 mol L⁻¹ Ca
226 solution. For instance, operating the 5% w w⁻¹ nitric acid, 20 g L⁻¹ S, 20 g L⁻¹ Cl
227 or 0.1 mol L⁻¹ Na at Q_g 0.3 L min⁻¹, the emission signal was 6-fold higher,
228 approximately, than at Q_g 0.9 L min⁻¹ in the wavelength range where the main
229 nitrogen molecular emission bands are located (i.e., 300-450 nm). This fact
230 indicates that a greater amount of solvent loaded into the plasma can cause a
231 deterioration of the plasma thermal conditions.[12] In the case of the organic
232 matrices, for the 20 g L⁻¹ C solution the emission signal was only 1.06-fold higher
233 on average at Q_g 0.3 L min⁻¹ with respect to that obtained at Q_g 0.9 L min⁻¹. This
234 less noticeable background difference is due to the fact that the emission of the
235 CN molecular band was so strong that it even saturated the detector. Conversely,

236 for the 0.25 mol L⁻¹ Ca solution an opposite behaviour was observed. As the main
237 emission signal was related to Ca atomic and ionic emission lines, the
238 background emission increased with the increase of the Q_g since a greater
239 amount of sample, and hence of Ca, reached the plasma. It is interesting to note
240 that, as well as the rest of the solutions, the main N-based molecular emission
241 bands (300-450 nm range) shown a decrease in the emission signal with the
242 increase of Q_g due to the deterioration of plasma conditions.

243 Because the complex background emission registered for some of the
244 matrices tested potential spectral interferences could occur on those elements
245 whose most sensitive emission line is located near to molecular emission bands
246 such as: Tm I 384.402, Gd II 385.097, Re I 386.046, Mo I 386.410 nm, Er II
247 390.631 and Ga I 417.204 nm operating organic solutions, or those lines located
248 above 370 nm (e.g., Sr II 407.771, Ga I 417.104 nm) when a saline solution is
249 introduced in the plasma (Fig. S3).

250

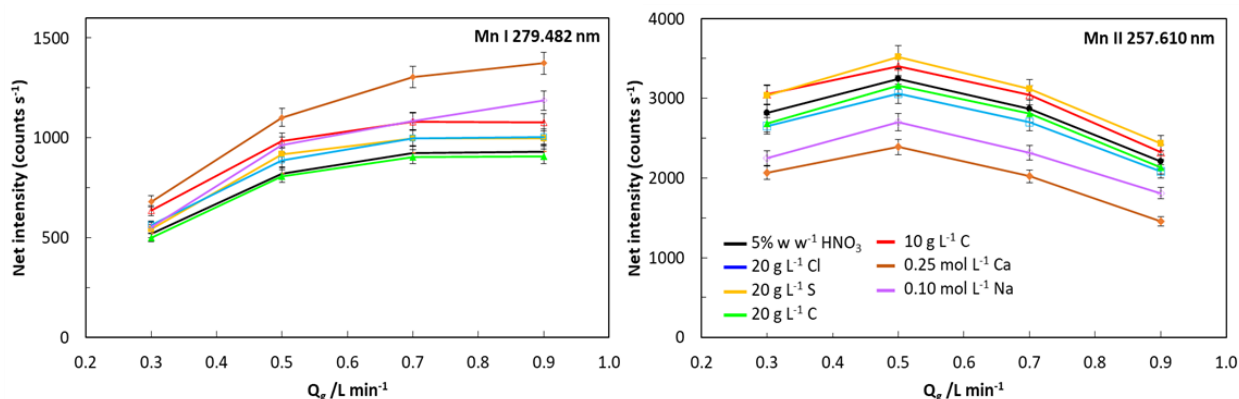
251 **3.2 Non-spectral interferences**

252 *3.2.1 Influence of the nebulizer gas flow rate*

253 It is well known that Q_g plays a significant role on both emission spectrum
254 and matrix effects in high-power (N₂)-MIP cavities.[12,13,37] Therefore, the
255 influence of Q_g was evaluated for a total of 41 emission lines (atomic and ionic)
256 of 19 elements (Ag, Al, As, B, Ca, Cd, Co, Cr, Cu, Fe, Ga, In, Mg, Mn, Ni, Pb, Sr,
257 Tl, and Zn) in the presence of the matrices selected. Fig. 2 shows the effect of Q_g
258 on the net emission signal of Mn I 279.482 nm and Mn II 257.610 nm for each
259 matrix and the reference solution. These lines were selected to show the different

260 behaviours observed in the presence of the matrices tested. The remaining lines
261 are included in the Supplementary material (Fig. S4). Mn I 279.482 nm emission
262 signal increased up to 0.7 L min⁻¹ where a plateau was reached for all the
263 matrices except for 0.25 mol L⁻¹ Ca and 0.10 mol L⁻¹ Na solutions. For the later
264 matrices, Mn I 279.482 nm emission signal continuously rose up with Q_g (the
265 emission signal increased an 8% approximately between 0.7 and 0.9 L min⁻¹). In
266 the case of Mn II 257.610 nm, a maximum was observed at a Q_g of 0.5 L min⁻¹
267 for all the matrices tested. Similar findings were registered for the rest of the
268 emission lines evaluated (Table S4). These results indicates that, conversely to
269 that observed for other high-power (N₂)-MIP,[12,13] the optimum Q_g for a given
270 wavelength with the MICAP is less affected by matrix characteristics. In general,
271 for MICAP, an optimal Q_g of 0.7 L min⁻¹ has been obtained for atomic lines and
272 0.5 L min⁻¹ for the ionic ones, regardless of the matrix considered (Table S4). On
273 the contrary, the data reported by Serrano et al. [12,13] operating a Hammer
274 cavity shown a greater variability between the optimum Q_g values obtained for
275 the different emission lines in the presence of the matrices evaluated. For
276 instance, in that study an optimum Q_g value of 0.6 L min⁻¹ was obtained for the
277 Mn II 257.610 nm emission line operating a 5% w w⁻¹ nitric acid whereas the
278 optimum one in the presence of saline solutions (i.e., 0.25 mol L⁻¹ Ca and 0.25
279 mol L⁻¹ Na) was 0.4 L min⁻¹. [13]

280



281
 282 **Fig. 2** Influence of the nebulizer gas flow rate (Q_g) on the net emission signal obtained
 283 for Mn I 279.482 nm and Mn II 257.610 nm in MICAP-OES operating different matrix
 284 solutions.
 285

286 Therefore, since the changes in the emission signal between Q_g 0.5 and 0.7
 287 L min⁻¹ were, in general, lower than 10% for almost all the emission lines tested
 288 in the presence of the different matrices evaluated, it is possible to select a
 289 compromise value of Q_g to take advantage of the multi-element capabilities
 290 offered by MICAP-OES. According to our data, Q_g 0.5 L min⁻¹ was selected as a
 291 compromise condition to avoid the deterioration of the plasma robustness, and
 292 sensitivity according to the data discussed previously (see section 3.1).

293 Regarding the analyte emission signal, it has been observed that different
 294 behaviours could be obtained depending on the characteristics of the lines (i.e.,
 295 atomic or ionic) and the matrices evaluated. Fig. 2 shown that Mn II 257.610 nm
 296 emission signal was negatively affected in the presence of 0.25 mol L⁻¹ Ca and
 297 0.1 mol L⁻¹ Na, irrespective of the Q_g . For instance, at Q_g 0.5 L min⁻¹ the emission
 298 signal was suppressed approximately 26 and 17%, with respect to the reference
 299 solution, in the presence of 0.25 mol L⁻¹ Ca and 0.1 mol L⁻¹ Na respectively. On
 300 the other hand, for the remaining matrices evaluated changes in the emission

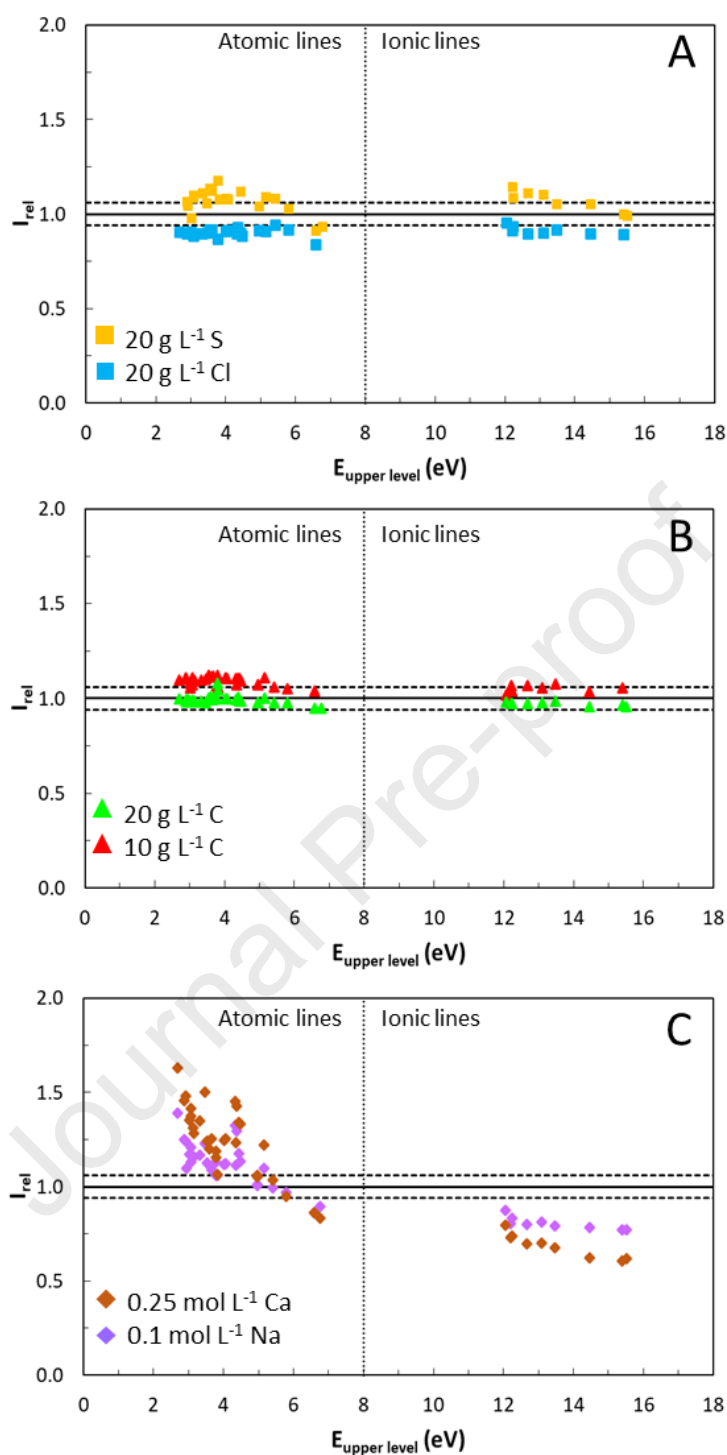
301 signals were between 5 – 8%, for 10 g L⁻¹ C and 20 g L⁻¹ S respectively, at Q_g 0.5
302 L min⁻¹ regarding the reference solution. Conversely, Mn I 279.482 nm signal was
303 increased by approximately 41% in the presence of 0.25 mol L⁻¹ Ca and a 17%
304 approximately with 0.1 mol L⁻¹ Na solution regarding the reference solution.
305 Similar behaviours were also obtained for the remaining (atomic and ionic) lines
306 investigated (Fig. S4). In general, it was observed that atomic lines, mainly those
307 with low E_{upper level} (e.g., Sr 460.733, Ag 328.068 and Al 394.401nm), defined as
308 the upper electronic level involved in the electron transition of each emission line,
309 shown positive matrix effects (i.e., signal enhancement) when operating Na and
310 Ca matrices. Conversely, those atomic emission lines with higher E_{upper level} values
311 and the ionic ones shown negative matrix effects (i.e., signal suppression).

312

313 3.2.2 Influence of the emission line characteristics

314 According to our data as well as previous works in the literature about non-
315 spectral interferences, it is self-evident that matrix effects on emission signal
316 depends on wavelength characteristics and, more specifically, on the E_{upper level}
317 values. For this reason, this matter has been examined in detailed to gain insight
318 into matrix effects origin with the MICAP.[13,39] Fig. 3 shows the influence of the
319 E_{upper level} on I_{rel} for the different emission lines selected in the presence of the
320 matrices selected. I_{rel} is defined as the net emission signal of the analyte obtained
321 in each matrix solution relative to that obtained for the 5% w w⁻¹ HNO₃ solution.
322 The signal repeatability for all the lines in the MICAP-OES was, mainly, about 3%
323 RSD (3 replicates). Hence, it could be considered that I_{rel} values below 0.94
324 indicates negative matrix effects (signal suppression) and above 1.06 positive

325 matrix effects (signal enhancement). In general, non-significant matrix effects
326 within experimental uncertainties (dashed lines in Fig. 3) were noticed for the
327 inorganic acid (Fig. 3A) and organic solutions (Fig. 3B). These results are similar
328 to those previously reported for high-power (N₂)-MIP cavities (i.e., Okamoto,[14]
329 Hammer,[12,15,13,40] MICAP, [21] Grand-MP [16]) in the presence of these
330 matrices. On the other hand, for saline matrices (Fig. 3C), it can be observed that
331 I_{rel} values decreased with $E_{upper\ level}$. Interestingly, a cross-over point between
332 positive and negative matrix effects was observed. Atomic lines with $E_{upper\ level} <$
333 4.5 eV shown positive matrix effects, whereas for atomic lines with higher E_{upper}
334 $level$ values and ionic emission lines negative matrix effects ($I_{rel} < 0.94$) prevailed
335 in the presence of both saline matrices (i.e., 0.25 mol L⁻¹ Ca and 0.1 mol L⁻¹ Na).
336 Moreover, as expected from the salt concentration, the magnitude of the matrix
337 effects was higher for the 0.25 mol L⁻¹ Ca solution than for the 0.1 mol L⁻¹ Na one.
338 These data contrast with those reported previously by Hallwirth et al. [27]
339 operating alkaline matrices. These authors reported significant matrix effects
340 mainly caused by alkaline elements even at concentration values as low as 20
341 mg mL⁻¹, but did not observed a correlation between the characteristics of the
342 emission line (i.e., E_{sum} , the sum of the excitation and ionization energy) and the
343 magnitude of matrix effects. These disagreements may be due to the different
344 working conditions and experimental setup used. Thus, both Q_g and Q_l were not
345 specifically optimized and experimental values were selected according to those



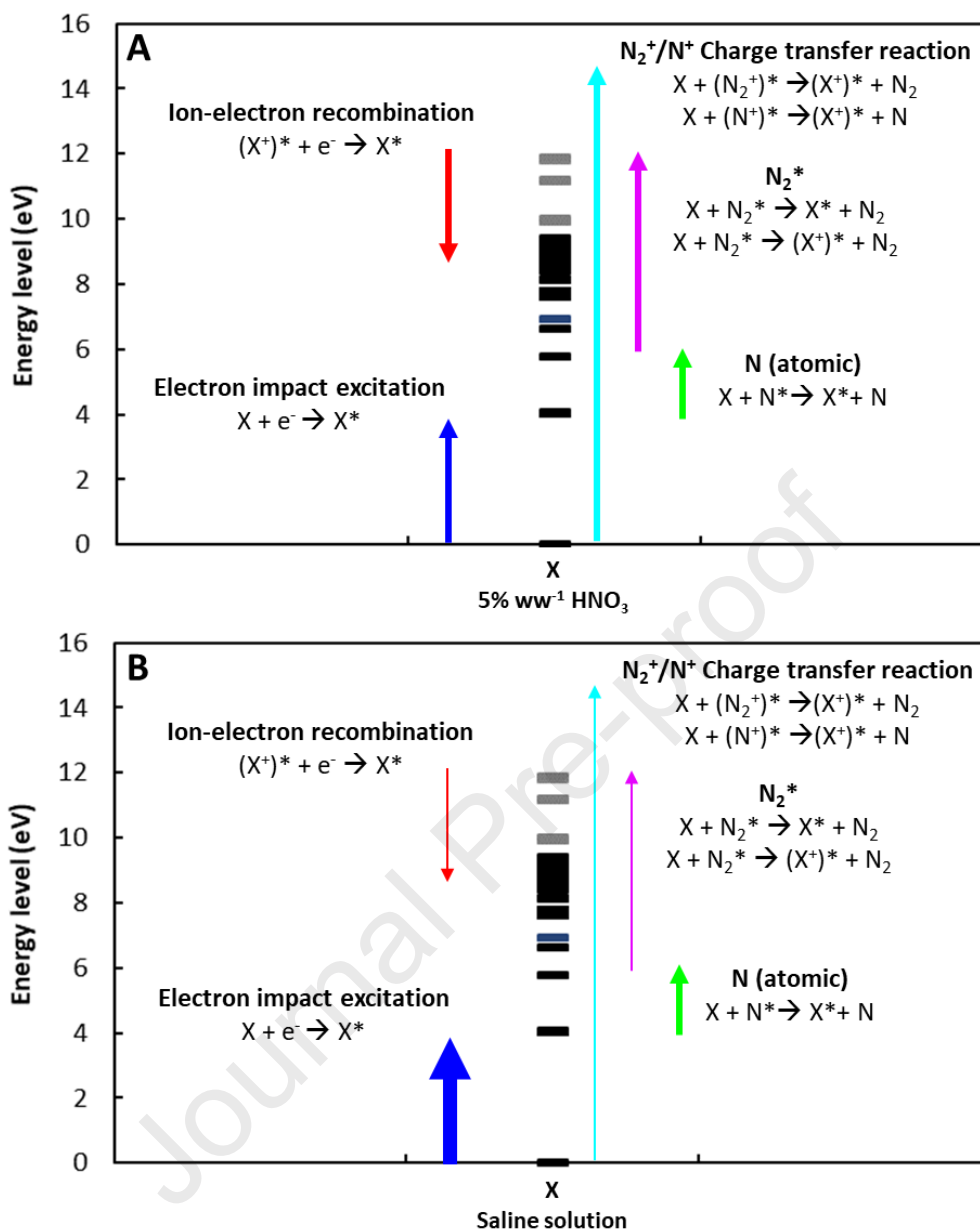
346

347 **Fig. 3** Influence of $E_{upper\ level}$ on the relative signal intensity (I_{rel}) obtained in the presence of
 348 of (A) inorganic acid matrices (i.e., 20 g L⁻¹ Cl, 20 g L⁻¹ S); (B) organic matrices (i.e., 20
 349 g L⁻¹ C and 0.43 mol L⁻¹ HOAc); and (C) saline matrices (i.e., 0.25 mol L⁻¹ Ca and 0.10
 350 mol L⁻¹ Na) regarding 5% w w⁻¹ nitric acid. Q_g 0.5 L min⁻¹; Q_l 0.3 ml min⁻¹. I_{rel} values
 351 among horizontal dotted lines indicated no matrix effects.
 352

353 commonly used in ICP-OES for routine analysis. On the other hand, the nebulizer
354 employed (i.e., Type A, Meinhard, USA) was not the most suitable for the analysis
355 of saline matrices. Nonetheless, the results obtained in the present work agreed
356 with other results reported in the literature for this plasma source [21,22,23] and
357 alternative high-power (N₂)-MIP cavities. [12,13,41,42] Nevertheless, it is
358 interesting to note that the magnitude of matrix effects registered in this work was
359 lower, for both positive ($I_{rel} > 1.06$) and negative ($I_{rel} < 0.94$) effects, regarding the
360 results reported operating a Hammer cavity using a similar experimental
361 arrangement (i.e., sample introduction system, optimum Q_g and matrix solution
362 composition).[13] For instance, the I_{rel} values obtained in the present work for the
363 Sr I 460.733 nm ($E_{upper\ level} = 2.69$ eV), which presented positive matrix effects, is
364 4.3 and 3.4-fold lower for a 0.25 mol L⁻¹ Ca and 0.1 mol L⁻¹ Na matrices,
365 respectively, with regard the I_{rel} values reported with the Hammer cavity.[13]
366 Conversely, for emission lines affected by negative matrix effects such as Mn II
367 257.610 nm ($E_{upper\ level} = 12.24$ eV), I_{rel} values are 1.2 and 1.3-fold higher for a
368 0.25 mol L⁻¹ Ca and 0.1 mol L⁻¹ Na matrices, respectively operating a MICAP-
369 OES. This fact indicates that MICAP is less prone to non-spectral interferences
370 in the presence of saline solutions than other high-power (N₂)-MIP cavities and,
371 hence, LoDs are less dependent on matrix characteristics. The instrumental LoD
372 values obtained in the presence of some saline matrices employed in elemental
373 bioavailability procedures (i.e., 0.01 mol L⁻¹ CaCl₂ and 0.1 mol L⁻¹ NaNO₃) (Table
374 S3) were similar to those obtained for a 5% w w⁻¹ nitric acid matrix (see Table
375 S5). Moreover, it is interesting to note that these LoDs were, in general, of the
376 same order of magnitude as those afforded by both ICP-OES and alternative

377 high-power (N₂)-MIP cavities.[22]

378 To explain experimental findings shown in Fig. 3C, it should be considered
379 how the introduction of saline matrices into the plasma affects the different
380 mechanisms involved in populating atomic and ionic electronic levels (Fig. 4). In
381 the absence of easily ionizable elements (Fig. 4.A), ionic levels are populated by
382 N₂⁺ and N⁺-based charge transfer reactions and the collision with metastable N₂^{*}
383 species. [43,44] On the other hand, atomic levels are mostly populated by three
384 different mechanisms, namely: (i) electron impact. This excitation pathway affects
385 the low energy atomic levels and depends on both the population of the atom
386 ground level and electronic density; (ii) ion-electron recombination. Unlike the
387 previous mechanism, it affects atomic levels of high energy and depends on both
388 ionic population and electron density; and (iii) collision with metastable atomic N^{*}
389 (²D and ²P levels) species. In this case, only atomic levels close to metastable N^{*}
390 (atomic) energy are affected (i.e., 4-5 eV) and it is independent of electron
391 density. [43,45] The introduction of easily ionizable elements into the plasma
392 causes an enhancement in the electron number density affecting a large part of
393 the above-mentioned mechanisms (Fig. 4B) and, hence, both atomic and ionic
394 emission. [12,13,21,41,42] An increase in plasma electron density shifts the
395 ionization equilibrium towards the formation of atoms. This means that the
396 population of analyte (X⁺) and nitrogen (N₂⁺ and N⁺) ions decrease whereas the
397 atomic ones increase. [12,13] According to this scheme, the signal increase
398 registered for the atomic lines with E_{upper level} < 4.5 eV can be explained
399 considering that the electron impact mechanism is favored (i.e., higher atomic
400 population and electron density impact). On the other hand, all the mechanisms



401

402 **Fig. 4** Simplified atomic (black) and ionic (grey) energy level diagram for an analyte
 403 showing potential excitation and ionization pathways operating (A) 5% w w⁻¹ nitric acid
 404 and (B) saline solutions. The thickness of the arrows indicates the relevance of the
 405 mechanism in each situation.

406

407 relying on ionic species (i.e., ion-electron recombination or N₂⁺-based charge
 408 transfer reactions) are less favored thus affecting negatively the emission signal
 409 of both ionic and atomic lines with E_{upper level} > 4.5 eV. On this regard, because

410 the decrease in the N_2^+ molecular emission band with the MICAP (Fig S5) is lower
411 than that previously reported for the Hammer cavity [12,13] (i.e., emission signal
412 decreased a 48% and a 80% in the presence of 0.25 mol L^{-1} Ca solution with
413 regard to the reference solution operating MICAP and Hammer cavity,
414 respectively), it is easier to understand why the magnitude of the matrix effects
415 for the MICAP are lower (i.e., higher plasma robustness). Finally, atomic
416 electronic levels with energy values between 4-6 eV are mostly populated by
417 collision with N metastable atoms [46] and they are expected to be less affected
418 by the introduction of easily ionizable elements. In fact, this behavior has also
419 been previously observed in high-power (N_2)-MIP plasmas, regardless the cavity
420 employed. [12,13,21,41,42]

421

422 3.2.3 Correction of matrix effects

423 Internal standardization (IS) is a widely employed calibration strategy to
424 mitigate matrix effects and improve analytical figures of merit (e.g., accuracy,
425 precision, long term performance, etc.) in atomic spectrometry. To date, different
426 IS have been successfully proposed for elemental analysis with MIPs, covering
427 either plasma molecular species (the N_2^+ and OH molecular emission band) [47]
428 or elements externally added to both samples and standards (i.e., Te, Co, Be,
429 Ga, In, Sc, Y, etc.). [48,49]. Nevertheless, because sequential spectrometers are
430 usually employed, [1,15] this strategy is not easy to apply for multi-elemental
431 determinations since the internal standard and the analytes of interest are not
432 measured simultaneously. For this reason, the purpose of the present study was

433 to evaluate the suitability of five different elements (i.e., Au, Pd, Rh, Sc and Y) as
434 IS, taking advance of the fact that MICAP-OES is equipped with a real-time
435 simultaneous spectrometer. The Au I 242.795, Rh I 369.236 and Pd I 340.458
436 nm lines were selected as potential IS to correct signal bias for atomic lines
437 whereas Sc II 424.682 and Y II 377.433 nm for the ionic ones.

438 To evaluate the suitability of the IS, a 5 mg kg⁻¹ multielemental solutions
439 containing 0.5 mg kg⁻¹ of each IS selected were prepared in two common saline
440 matrices employed in elemental bioavailability procedures (i.e., 0.01 mol L⁻¹
441 CaCl₂, 0.1 mol L⁻¹ NaNO₃) (Table S3)[13] and in 5% w w⁻¹ nitric acid. Table 2
442 shows the emission signal ratio obtained for different elements and emission
443 lines, selected to cover the E_{upper level} range evaluated in previous sections, and
444 the IS in the presence of saline solutions relative to that obtained for the 5% w w⁻¹
445 ¹ HNO₃ solution. As it can be observed, the signal ratio in the presence of both
446 saline solutions was between 0.74 and 1.37 (i.e., an average 1.05 of signal bias)
447 for the analytes and IS emission lines selected, with the exception of Au for which
448 a higher signal bias was obtained (about 50-60%) for both matrices. This fact may
449 be due to during the preparation of the multielement solutions with the addition of
450 Au, a precipitate appeared. These results were comparable to those reported for
451 similar matrix solutions operating a Hammer cavity instrument equipped with a
452 sequential spectrometer.[13] Hence, Rh, Pd, Sc and Y, could be used in the
453 present work as IS to correct signal bias for atomic and ionic emission lines in the
454 analysis of different CRMs.

455

456

457

458

459

460

Table 2. Signal ratio obtained for saline solutions (i.e., 0.01 mol L⁻¹ CaCl₂ and 0.1 mol L⁻¹ NaNO₃) in comparison with 5% w w⁻¹ nitric acid for a 5 mg kg⁻¹ multielemental solution. Q_g 0.5 L min⁻¹ and Q_l 0.3 mL min⁻¹.

	Emission line (nm)	E _{upper level} (eV)	0.01 mol L ⁻¹ CaCl ₂	0.1 mol L ⁻¹ NaNO ₃
Analytes	Sr I 460.733	2.69	1.19	1.37
	Cr I 425.435	2.91	0.97	1.18
	Pb I 405.781	4.38	1.01	1.20
	Zn I 213.857	5.80	1.14	0.90
	Mg II 280.271	12.06	1.07	0.84
	Mn II 257.610	12.24	1.08	0.89
	Cd II 226.501	14.46	1.07	0.74
IS	Rh I 369.236	3.36	1.03	1.09
	Pd I 340.458	4.45	n.d.	1.09
	Au I 242.795	5.11	1.56	1.61
	Sc II 424.682	9.79	1.00	0.76
	Y II 377.433	9.97	1.04	0.82

461

*n.d. not determined

462

463 3.3 Analysis of complex matrix samples

464

465

466

467

468

469

470

471

472

To evaluate the analytical capabilities of the MICAP-OES when dealing with complex samples, several CRMs covering a wide range of sample concomitants (i.e., environmental, food, and polymers) were analysed. The CRM-DW1 Drinking water was analysed directly while BCR-146 Sewage sludge industrial, BCR-185 Bovine liver, BCR-278R Mussel tissue, NIST-1549 Non-fat milk powder and ERM-EC681k Polyethylene (high level) materials were analysed after an acid digestion treatment. On the other hand, for the BCR-483 Sewage sludge amended soil four different extractions (i.e., 0.05 mol L⁻¹ Na₂EDTA, 0.43 mol L⁻¹ acetic acid, 0.01 mol L⁻¹ CaCl₂ and 0.1 mol L⁻¹ NaNO₃) were performed

473 for the elemental extraction in each soil fraction according to the standardized
474 protocol indicated in the CRM report (Table S3). Sample analysis was carried out
475 using a single set of experimental parameters (i.e., Q_g 0.5 L min⁻¹) and a
476 calibration procedure based on matrix matched standard with Rh and Sc as IS.
477 Method validation was performed according to the European conformity
478 guidelines concerning the performance of analytical methods and the
479 interpretation of results [50] and different international guidance protocols for the
480 analysis of environmental samples. [51,52,53]

481

482 3.3.1 Limits of detection

483 Method limits of detection ($mLODs$) were estimated according to the IUPAC
484 guidelines [54] using the calibration curve and the most sensitive wavelength of
485 each analyte. The dilution factor (sample mass:final weight) for the sample
486 digestion and the solid:liquid ratio of each extraction procedure were taken into
487 account. It is interesting to note that it was not possible to use the two most
488 sensitive emission lines for Ca (i.e., Ca II 393.366 and Ca II 396.847 nm) in the
489 presence of the 0.43 mol L⁻¹ HOAc extraction solution (i.e., 10 g L⁻¹ C
490 approximately), since both wavelengths were located near the 380-390 nm range
491 which is interfered by carbon-based molecular emission bands. Thus, the third
492 most intense emission line (Ca I 422.673 nm) was used to estimate the $mLODs$ for
493 this matrix instead. Table 3 gathers the $mLODs$ obtained expressed as mg kg⁻¹
494 dry weight (n=3) for the different CRMs analyzed. In general, $mLODs$ were of the
495 same order of magnitude for all the elements evaluated, except those obtained
496 for the digested CRMs and the 0.43 mol L⁻¹ HOAc extraction solution, for which

497 mLODs were one order of magnitude higher. This fact was related to the
498 differences in the dilution factor applied and to the changes in the background
499 signal caused by the presence of carbon. In the case of the analyte Ca, as a less
500 sensitive emission line was used to estimate the mLODs for the 0.43 mol L⁻¹ HOAc
501 extraction solution, the value obtained was higher than those obtained for the rest
502 of the extraction solutions, but of the same order of magnitude regarding the
503 mLODs values obtained for the digested CRMs. The mLODs values obtained in
504 this work were similar to those reported operating alternative high-power (N₂)-
505 MIP cavities with solutions of similar composition, especially those obtained for
506 the BCR-483 Sewage sludge amended soil were of the same order of magnitude
507 that those previously reported operating a Hammer cavity. [13,55,56]

508

509 3.3.2 *Trueness*

510 Table 4 shows elemental recoveries for those elements analysed in the
511 different CRMs. In accordance with different international guidance protocols,
512 [50,51,52,53] the accuracy of the measurements of a CRM is successfully
513 assessed when the deviation of the analyte concentration values determined
514 experimentally and those certified for each CRM not lie outside the limit $\pm 10\%$.
515 As it can be observed, in general, quantitatively recovery values (between 90 and
516 110%) were obtained for all the analytes tested irrespective of the CRM
517 considered, with the exception of the BCR-483 Sewage sludge amended soil. For
518 this CRM, recovery values outside $\pm 10\%$ range were obtained for Cr and Zn in
519 the EDTA and CaCl₂ extraction solutions, respectively. Lastly, it is interesting to
520 note that concentration values for all the analytes evaluated in the NaNO₃

521 extraction fraction could not be registered due to their low concentration levels.

522

523 3.3.3 *Precision and robustness*

524 To evaluate the repeatability of the methods tested (intra-day precision), six
525 replicates of each sample were analysed on the same day. For each element,
526 the relative standard deviation (RSD%) varied between 1 and 6% depending on
527 the CRM. Finally, as regards the reproducibility (inter-day precision), it was
528 evaluated analysing five replicates of each sample in four different days, and it
529 was lower than 8% for all the samples tested.

530

531 4. **Conclusions**

532 This work shows that MICAP-OES is a suitable system for the elemental
533 analysis of complex matrix samples. Unlike other high-power (N₂)-MIP cavities
534 (i.e., Okamoto, Hammer, Grand-MP), plasma optimization is more
535 straightforward since, irrespective of the emission line and matrix characteristics,
536 a single Q_g can be selected for the simultaneous analysis of different elements.
537 On the other hand, it has been observed that this system provides a more robust
538 discharge. Irrespective of the emission line considered, no matrix effects were
539 observed when operating acid and organic solutions. Even though this system is
540 still prone to matrix effects caused by easily ionizable elements, changes on both
541 atomic and ionic emission are significantly lower than those traditionally reported
542 for microwave plasmas. In any case, non-spectral interferences by sample
543 concomitants, could be appropriately addressed by means of real-time internal
544 standardization and without compromising sample throughput. Our data shows

545 that there is not a universal IS to correct matrix effects and improve long-term
546 performance thus requiring two internal standards to correct matrix effects for
547 atomic (i.e., Rh or Pd) and ionic (i.e., Sc and Y) emission lines.

548

549 **Acknowledgements**

550 This research was funded by the University of Alicante through research
551 projects VIGROB-050.

Journal Pre-proof

Table 3. Method limits of detection (mLODs) expressed as mg kg⁻¹ dry weight (n=3) in MICAP-OES for the different CRMs evaluated. Q_g 0.5 L min⁻¹ and Q_l 0.3 mL min⁻¹.

Matrices	CRM-DW1 Drinking water	Digested CRMs	BCR-483 Sewage sludge amended soil			
			0.43 mol L ⁻¹	0.10 mol L ⁻¹	0.05 mol L ⁻¹	0.01 mol L ⁻¹
			¹ HOAc	¹ NaNO ₃	¹ EDTA	¹ CaCl ₂
Cr 425.435	0.05	3	2	0.13	0.7	1
Al 396.152	0.04	5	1.2	0.15	0.03	0.15
Ni 352.454	0.08	20	1.3	0.15	1.2	2
Ag 328.068	0.17	90	2	0.53	8	n.d.
Cu 324.754	0.01	9	0.2	0.05	1.0	0.4
Pb 405.781	0.01	12	5	0.25	0.9	1.2
Cd 228.802	0.01	2	1.2	0.25	0.3	0.3
Zn 213.587	0.01	7	1	0.25	0.2	0.6
Ba 493.408	0.01	2	0.3	0.05	0.4	0.3
Ca 393.366	0.05	1	3*	0.07	0.6	n.d.
Mg 280.270	0.01	1	1.4	0.03	0.2	0.9
Mn 257.610	0.02	3	0.7	1.00	0.1	0.2
Fe 259.940	0.03	2	1	0.18	0.1	0.2
Co 238.892	0.03	13	10	1.50	0.4	1.7

*LoD value calculated for the emission line 422.673 nm.

n.d.: not determined

Table 4. Analyte percent recoveries (mean \pm SD, n=3) obtained for the different certified reference materials analysed by MICAP-OES. Q_g 0.5 L min^{-1} and Q_l 0.3 mL min^{-1} .

Elements	CRM-DW1	BCR-146R	BCR-185R	BCR-278R	NIST-1549	ERM-EC681k	BCR-483 Sewage sludge amended soil		
	Drinking water	Sewage sludge industrial	Bovine Liver	Mussel tissue	Non-fat milk powder	Polyethylene (high level)	EDTA	HOAc	CaCl ₂
Ca	82.6 \pm 1.2	-	-	-	90 \pm 3	-	-	-	-
Cd	< LoDs	90 \pm 20	< LoDs	< LoDs	< LoDs	90 \pm 2	98.8 \pm 0.7	88 \pm 4	< LoDs
Cr	< LoDs	92 \pm 7	-	< LoDs	< LoDs	< LoDs	170 \pm 15	92 \pm 2	< LoDs
Cu	102 \pm 4	91 \pm 4	89 \pm 2	< LoDs	< LoDs	-	90 \pm 4	98 \pm 5	< LoDs
Fe	111 \pm 5	-	-	-	< LoDs	-	-	-	-
Mg	112 \pm 3	-	-	-	92 \pm 12	-	-	-	-
Mn	< LoDs	87 \pm 4	101 \pm 3	95 \pm 6	< LoDs	-	-	-	-
Na	103.7 \pm 0.2	-	-	-	102.35 \pm 0.11	-	-	-	-
Ni	< LoDs	< LoDs	-	-	-	-	106 \pm 5	< LoDs	< LoDs
P	-	-	-	-	109 \pm 5	-	-	-	-
Pb	< LoDs	91 \pm 6	< LoDs	< LoDs	< LoDs	108 \pm 10	85 \pm 9	< LoDs	< LoDs
Zn	< LoDs	103 \pm 5	96 \pm 3	98.5 \pm 1.5	113 \pm 17	101 \pm 2	94 \pm 2	98 \pm 5	145 \pm 1

References

- [1] A. Muller, D. Pozebon, V. L. Dressler, Advances of nitrogen microwave plasma for optical emission spectrometry and applications in elemental analysis: a review, *J. Anal. At. Spectrom.* 35 (2020) 2113-2131.
- [2] B. M. Fontoura, F. C. Jofré, T. Williams, M. Savio, G. L. Donati, J. A. Nóbrega, Is MIP-OES a suitable alternative to ICP-OES for trace elements analysis?, *J. Anal. At. Spectrom.*, 37 (2022) 966-984.
- [3] V. Sreenivasulu, N. S. Kumar, V. Dharmendra, M. Asif, V. Balaram, H. Zhengxu, Z. Zhen, Determination of boron, phosphorus, and molybdenum content in biosludge samples by microwave plasma atomic emission spectrometry (MP-AES), *Appl. Sci.* 7 (2017) 264-273.
- [4] F. C. Jofré, M. Perez, N. Kloster, M. Savio, Analytical methods assessment for exchangeable cations analysis in soil: MIP OES appraisalment, *Commun. Soil. Sci. Plant* 51 (2020) 2205–2214.
- [5] E. Baranyai, C. N. Tóth, I. Fábian, Elemental analysis of human blood serum by microwave plasma – Investigation of the matrix effects caused by sodium using model solutions, *Biol. Trace. Elem. Res.* 194 (2020) 13-23.
- [6] C. B. Williams, T. G. Wittmann, T. McSweeney, P. Elliott, B. T. Jones, G. L. Donati, Dry ashing and microwave-induced plasma optical emission spectrometry as fast and cost-effective strategy for trace element analysis, *Microchem. J.* 132 (2017) 15-19.

- [7] N. Ozbek, H. Tinas, A. E. Atespare, A procedure for the determination of trace metals in rice varieties using microwave induced plasma atomic emission spectrometry, *Microchem. J.* 144 (2019) 474-478.
- [8] D. A. Goncalves, T. McSweeney, M. C. Santos, B. T. Jones, G. L. Donati, Standard dilution analysis of beverages by microwave-induced plasma optical emission spectrometry, *Anal. Chim. Acta* 909 (2016) 24-29.
- [9] S. M. Azcarate, L. P. Langhoff, J. M. Camiña, A green single-tube sample preparation method for wear metal determination in lubricating oil by microwave induced plasma with optical emission spectrometry, *Talanta* 95 (2019) 573-579.
- [10] J. Nelson, G. Gilleland, L. Poirier, D. Leong, P. Hajdu, F. Lopez-Linares, Elemental analysis of crude oils using microwave plasma atomic emission spectroscopy, *Energy fuels* 29 (2015) 5587-5594.
- [11] T. L. Espinoza Cruz, M. Guerrero Esperanza, K. Wrobel, E. Y. Barrientos, F. J. Acevedo Aguilar, K. Wrobel, Determination of major and minor elements in Mexican red wines by microwave-induced plasma optical emission spectrometry, evaluating different calibration methods and exploring potential of the obtained data in the assessment of wine provenance, *Spectrochim. Acta B* 164 (2020), 105754.
- [12] R. Serrano, G. Grindlay, L. Gras, J. Mora, Evaluation of calcium-, carbon- and sulfur-based non-spectral interferences in high-power MIP-OES: comparison with ICP-OES, *J. Anal. At. Spectrom.* 34 (2019) 1611–1617.

- [13] R. Serrano, E. Anticó, G. Grindlay, L. Gras, C. Fontàs, Determination of elemental bioavailability in soils and sediments by microwave induced plasma optical emission spectrometry (MIP-OES): Matrix effects and calibration strategies, *Talanta* 240 (2022) 123166.
- [14] Z. Zhang, K. Wagatsuma, Effects of easily ionizable elements and nitric acid in microwave-induced nitrogen plasma atomic emission spectrometry, *Spectrochim. Acta Part B* 57 (2002) 1247–1257.
- [15] C. B. Williams, R. S. Amais, B. M. Fontoura, B. T. Jones, J. A. Nóbrega, G. L. Donati, Recent developments in microwave-induced plasma optical emission spectrometry and applications of a commercial Hammer-cavity instrument, *Trends Anal. Chem.* 116 (2019) 151–157.
- [16] E. V. Polyakova, Y. N. Nomerotskaya, A. I. Saprykin, Effect of matrix elements and acid on analytical signals in nitrogen microwave-plasma atomic emission spectrometry, *J. Anal. Chem.* 75 (2020) 474-478.
- [17] J. Jevtic, A. Menon and V. Pikelja, PCT/US2014/024312, WO2014159590 A2014159591, World Intellectual Property Organization, 2014.
- [18] J. Jevtic, A. Menon and V. Pikelja, PCT/US2014/024306, WO2014159588 A2014159581, World Intellectual Property Organization, 2014.
- [19] J. Jevtic, A. Menon and V. Pikelja, Presented at SCIX, Milwaukee, WI, 2013.
- [20] J. Jevtic, A. Menon and V. Pikelja, Presented at ICOPS/BEAMS 2014, Washington, DC, 2014.

- [21] K. M. Thaler, A. J. Schwartz, C. Haisch, R. Niessner, G. M. Hieftje, Preliminary survey of matrix effects in the Microwave-sustained, Inductively Coupled Atmospheric-pressure Plasma (MICAP), *Talanta* 180 (2018) 25-31.
- [22] A. J. Schwartz, Y. Cheung, J. Jevtic, V. Pikelja, A. Menon, S. T. Ray, G. M. Hietje, New inductively coupled plasma for atomic spectrometry: the microwave-sustained, inductively coupled, atmospheric-pressure plasma (MICAP), *J. Anal. At. Spectrom.* 31 (2016) 440-449.
- [23] H. Wiltsche, M. Wolfgang, Merits of microwave plasmas for optical emission spectrometry – characterization of an axially viewed microwave-sustained, inductively coupled, atmospheric-pressure plasma (MICAP), *J. Anal. At. Spectrom.*, 35 (2020) 2369-2377.
- [24] M. Schild, A. Gundlach-Graham, A. Menon, J. Jevtic, V. Pikelja, M. Tanner, B. Hattendorf, D. Günter, Replacing the argon ICP: Nitrogen microwave inductively coupled atmospheric-pressure plasma (MICAP) for mass spectrometry, *Anal. Chem.* 90 (2018) 13443-13450.
- [25] Z. You, A. Akkus, W. Weisheit, T. Giray, S. Penk, S. Buttler, S. Recknagel, C. Abad, Multielement analysis in soils using nitrogen microwave inductively coupled atmospheric-pressure plasma mass spectrometry, *J. Anal. At. Spectrom.* 37 (2022) 2556-2562.
- [26] A. Winckelmann, J. Roik, S. Recknagel, C. Abad, Z. You, Investigation of matrix effects in nitrogen microwave inductively coupled atmospheric pressure

plasma mass spectrometry (MICAP-MS) for trace element analysis in steels, *J. Anal. At. Spectrom.* 38 (2023) 1253-1260.

[27] F. Hallwirth, M. Wolfgang and H. Wiltsche, Matrix effects in simultaneous microwave induced plasma optical emission spectrometry: new perspective on an old problem, *J. Anal. At. Spectrom.* 38 (2023) 1682-1690.

[28] J. Entwisle, R. Hearn, Development of an accurate procedure for the determination of arsenic in fish tissues of marine origin by inductively coupled plasma mass spectrometry, *Spectrochim. Acta B* 61 (2006) 438–443.

[29] E. M. Seco-Gesto, A. Moreda-Piñeiro, A. Bermejo-Barrera, P. Bermejo-Barrera, Multi-element determination in raft mussels by fast microwave-assisted acid leaching and inductively coupled plasma-optical emission spectrometry, *Talanta* 72 (2007) 1178–1185.

[30] A. Durand, Z. Chase, A. T. Townsend, T. Noble, E. Panietz, K. Goemann, Improved methodology for the microwave digestion of carbonate-rich environmental samples, *Int. J. Environ. Anal. Chem.* 96 (2016) 119–136.

[31] A. Sahuquillo, J. F. López-Sánchez, R. Rubio, G. Rauret, R. P. Thomas, C. M. Davidson, A. M. Ure, Use of a certified reference material for extractable trace metals to assess sources of uncertainty in the BCR three-stage sequential extraction procedure, *Anal. Chim. Acta* 382 (1999) 317–327.

[32] Ph. Quevauviller, A. Ure, H. Muntau, B. Griepink, Improvement of Analytical Measurements within the BCR-Programme: Single and Sequential Extraction

Procedures Applied to Soil and Sediment Analysis, *Int. J. Environ. Anal. Chem.* 51 (1993) 129–134.

[33] J. L. Todolí, J. M. Mermet, Acid interferences in atomic spectrometry: analyte signal effects and subsequent reduction, *Spectrochim. Acta Part B* 54 (1999) 895–929.

[34] A. B. S. Silva, J. M. Higuera, C. E. M. Braz, R. C. Machado, A. R. A. Nogueira, Evaluation of different nebulizers performance on microwave-induced plasma optical emission spectrometry, *Spectrochim. Acta Part B* 168 (2020), 105867.

[35] N. Chalyavi, P. S. Doidge, R. J. S. Morrison, G. B. Partridge, Fundamental studies of an atmospheric-pressure microwave plasma sustained in nitrogen for atomic emission spectrometry, *J. Anal. At. Spectrom.* 32 (2017) 1988-2002.

[36] K. J. Jankowski, E. Reszke, *Microwave induced plasma analytical spectrometry*, Royal Society of Chemistry, Cambridge, 2011.

[37] R. Serrano, G. Grindlay, P. Niedzielski, L. Gras, J. Mora, Evaluation of MIP-OES as a detector in DLLME procedures: application to Cd determination in water samples, *J. Anal. At. Spectrom.* 35 (2020) 1351-1359.

[38] A. Kramida, Yu. Ralchenko, J. Reader, and NIST ASD Team (2022). NIST Atomic Spectra Database (ver. 5.10) (Last access July 2023): <https://physics.nist.gov/asd>.

[39] R. Serrano, G. Grindlay, L. Gras, J. Mora, Insight into the origin of carbon matrix effects on the emission signal of atomic lines in inductively coupled plasma

optical emission spectrometry, *Spectrochim. Acta Part B* 177 (2021), 106070.

[40] E.V. Polyakova, O.V. Pelipasov, Plasma molecular species and matrix effects in the Hummer cavity microwave induced plasma optical emission spectrometry, *Spectrochim. Acta Part B* 173 (2020) 105988.

[41] O. V. Pelipasov, E. V. Polyakova, Matrix effects in atmospheric pressure nitrogen microwave induced plasma optical emission spectrometry, *J. Anal. At. Spectrom.* 35 (2020) 1389–1394.

[42] K. Jankowski, K. Dreger, Study of an effect of easily ionizable elements on the excitation of 35 elements in an Ar-MIP system coupled with solution nebulization, *J. Anal. Atomic Spectrom.* 15 (2000) 269–274.

[43] G.C. Chan, G.M. Hieftje, Using matrix effects as a probe for the study of the charge-transfer mechanism in inductively coupled plasma-atomic emission spectrometry, *Spectrochim. Acta Part B* 59 (2004) 163–183.

[44] S.A. Lehn, G.M. Hieftje, Experimental evaluation of analyte excitation mechanisms in the inductively coupled plasma, *Spectrochim. Acta Part B* 58 (2003) 1821–1836.

[45] K. Wagatsuma, K. Satoh, Estimation using an enhancement factor on non local thermodynamic equilibrium behavior of high-lying energy levels of neutral atom in argon radio-frequency inductively-coupled plasma, *Anal. Sci.* 32 (2016) 535–541.

[46] R. Singh, Sisir Kumar Mitra, Scientific achievements and the fellowship of

the royal society of London, *Indian J. Hist. Sci.*, 52 (2017) 407-419.

[47] K. L. Lowery, T. McSweeney, S. P. Adhikari, A. Lachgar, G. L. Donati, Signal correction using molecular species to improve biodiesel analysis by microwave induced plasma optical emission spectrometry, *Microchem. J.* 129 (2016) 58–62.

[48] A. B. S. Silva, J. M. Higuera, A. R. A. Nogueira, Internal standardization and plasma molecular species: signal correction approaches for determination of phosphorus from phospholipids in meat by MIP-OES, *J. Anal. At. Spectrom.* 34 (2019) 782-787.

[49] L. N. Pires, F. S. Dias, L. S.G. Teixeira, Assessing the internal standardization of the direct multi-element determination in beer samples through microwave-induced plasma optical emission spectrometry, *Anal. Chim. Acta* 1090 (2019) 31-38.

[50] 2002/657/EC: Commission Decision of 12 August 2002 implementing Council Directive 96/23/EC concerning the performance of analytical methods and the interpretation of results.

[51] Canadian Council of Ministers of the Environment, Guidance manual for environmental site characterization in support of environmental and human health risk assessment, Volume 4 Analytical Methods, vol. 1557, PN, 2016, ISBN 978-1-77202-032-8.

[52] International Atomic Energy Agency, Soil sampling for environmental contaminants, IAEA, Vienna, 2004, ISBN 92-0-111504-0.

[53] Environmental Protection Agency (EPA), EPA/600/R-96/055 Guidance for the Data Quality Objectives Process EPA QA/G-4, 1994.

[54] J. Inczédy, T. Lengyel, A. M. Ure, A. Gelencsér, A. Hulanicki, IUPAC Analytical chemistry division, Compendium of analytical nomenclature, third ed., Blackwell, Oxford, 1998.

[55] F. C. Jofré, D. N. Larregui, V. N. Murcia, P. Pacheco, M. Savio, Infrared assisted digestion used as a simple green sample preparation method for nutrient analysis of animal feed by microwave induced plasma atomic emission spectrometry, *Talanta* 231 (2021) 122376.

[56] M. S. Lemos, K. G. F. Dantas, Evaluation of the use of diluted formic acid in sample preparation for elemental determination in crustacean samples by MIP-OES, *Biol. Trace Elem. Res.* 201 (2023) 3513-3519.

Highlights

- MICAP-OES is a suitable technique for elemental analysis of complex matrix samples.
- A single Q_g can be used regardless of wavelength and the sample matrix nature.
- Inorganic acid and organic solutions do not cause significant matrix effects.
- MICAP-OES is still prone to easily ionizable elements (EIEs) matrix effects.
- Real-time simultaneous internal standard can be used to mitigate EIEs matrix effects.

Declaration of interests

The authors declare that they have no known competing financial interests or personal relationships that could have appeared to influence the work reported in this paper.

The authors declare the following financial interests/personal relationships which may be considered as potential competing interests:

Journal Pre-proof